CMS Physics Analysis Summary

Contact: cms-pag-conveners-susy@cern.ch 2013/11/02

Search for supersymmetry in pp collisions at a center-of-mass energy of 8 TeV in events with two opposite sign leptons, large number of jets, b-tagged jets, and large missing transverse energy

The CMS Collaboration

Abstract

Results are reported from a search for new physics in pp collisions at $\sqrt{s} = 8$ TeV using a dataset corresponding to a total integrated luminosity of 19.7 fb^{-1} collected with the CMS experiment. Events with two opposite sign leptons, a large number of jets, b-tagged jets, and large missing transverse energy are used to search for new physics resulting in multiple top quarks and missing transverse energy in the final state. An entirely data-driven technique is used to estimate the standard model background, and the results are interpreted in the context of a sypersymmetric model in which pair produced gluinos decay to a pair of top quarks and a neutralino.

1 Introduction

One of the most natural extensions of the standard model (SM) of particle physics is supersymmetry (SUSY) [1–8]. Supersymmetry allows for gauge coupling unification at the energy of 10^{16} GeV, provides a good dark matter candidate (lightest supersymmetric particle, LSP), is a necessary component to explain quantum gravity in the framework of string theory, and automatically cancels the quadratic divergences in radiative corrections to the Higgs boson mass. For every particle in the standard model, SUSY introduces a super-partner, the "sparticle", with spin differing by 1/2 unit from the SM particle. There are theoretical arguments that suggest sparticle masses could be less than $\sim$ 1 TeV [7, 8] making the experiments at the Large Hadron Collider (LHC) an ideal place for their discovery.

With the successful 2012 LHC run, an integrated luminosity of 19.7 fb^{-1} in pp collisions at 8 TeV center-of-mass energy has been collected with the Compact Muon Solenoid (CMS) experiment. Events with two opposite-sign leptons (electrons or muons), a large number of jets, b-tagged jets, and large missing transverse energy ($\not\!\!E_{\mathrm{T}}$), are used to search for new physics with multiple top quarks and undetected particles in the final state. An entirely data-driven technique is used to estimate the standard model background, and the results are interpreted in the context of a simplified model scenario (SMS) [9–11] in which pair produced gluinos decay to a pair of top quarks and a neutralino ($\tilde{\mathrm{g}} \to \mathrm{t\bar{t}}\tilde{\chi}_1^0$), yielding four top quarks in the final state and two LSPs, and denoted as "T1tttt".

2 Event Samples, Trigger and Event Selection

Events are selected requiring the presence of at least two leptons, either two muons or two electrons or a muon-electron pair, recorded with dedicated dilepton triggers. In the case of the double-muon (electron) trigger, the selection is asymmetric with a transverse momentum,p_{T}, (energy of a cluster in the electromagnetic calorimeter) threshold of 17 GeV for the leading, higher-p_{T}, muon (electron) and 8 GeV for the sub-leading one. For the muon-electron trigger, the threshold on p_{T},(transverse energy, E_{T}) is 8 GeV (17 GeV) for the muon (electron). For all triggers, additional identification and isolation criteria are also applied.

Muon candidates are reconstructed by combining the information from the inner tracking system, the calorimeters, and the muon system [12]. Electron candidates are reconstructed by combining the information from the electromagnetic calorimeter (ECAL) with the silicon tracker, using shower shape and track-ECAL-cluster matching variables in order to increase the sample purity [13]. Jets are reconstructed using the anti-k_{T} clustering algorithm [14] with a distance parameter $\Delta R = \sqrt{(\Delta\phi)^2 + (\Delta\eta)^2} = 0.5$, with η being the pseudorapidity of the jet. The inputs to the jet clustering algorithm are the four-momentum vectors of reconstructed particles. Each such particle is reconstructed with the particle-flow technique that combines information from several sub-detectors [15]. The measured particle-flow (PF) jet transverse momenta are corrected with scale factors derived from simulation; to correct for any differences in the energy response between simulation and data, a residual correction factor derived from the latter is applied to jets in the data [16]. In general, $\not\!\!E_{\mathrm{T}} \equiv |\sum \vec{p}_{\mathrm{T}}|$, where the sum is taken over all final-state particles reconstructed in the CMS detector.

Simulated samples of the $\mathrm{t\bar{t}}$, Drell-Yan, W+jets, ttZ and ttW processes, as well as signal SMS samples, are produced using the MADGRAPH 4.4.24 [17] generator. The PYTHIA 6.4.22 [18] generator is used (using underlying event tune Z2* which is identical to the Z1 tune [19] except that Z2* uses the CTEQ6L [20] parton distribution functions (PDF) while Z1 uses CTEQ5L) to simulate the QCD, WW, ZZ, and WZ processes. Events are then processed with a simulation

of the CMS detector response based on GEANT4 [21]. Multiple proton-proton interactions are superimposed on the hard collision, and all simulated event samples are re-weighted according to the distribution of the number of primary vertices in data. Simulated events are reconstructed and analyzed in the same way as data events. Non-collision backgrounds are removed by applying quality requirements on the reconstructed primary vertex [22].

Events are required to have at least two opposite-sign leptons with $p_T > 20$ GeV and $|\eta| < 2.4$, and at least two jets with $p_T > 30$ GeV and $|\eta| < 2.4$. Jets are required to satisfy the quality criteria described in [23]. Leptons are selected following standard CMS quality criteria, and are required to be isolated from significant energy deposits and tracks in a cone of radius $\Delta R = 0.3$ around the direction of the lepton, with the relative isolation criterion set to be < 0.2. The lepton isolation is computed using particle-flow information [15]. An event-by-event correction is made to account for the effect of multiple pp interactions in the same bunch crossing (pileup). This correction subtracts the estimated contribution from pileup from the measured sum-p_T in the isolation cone. This contribution is of order 1 GeV, and it is calculated based on a measurement of the hadronic event activity not associated with the pp interaction that produced the leptons. For b-tagging of the PF jets, the combined secondary vertex method [24], which is based on the combination of secondary-vertex reconstruction and track-based lifetime information, is used at the "medium" working point, which has a 70% b-jet tagging efficiency and a probability of 1.5% to misidentify light-quark jets.

3 Signal Selection

In order to define the signal region, i.e. the region in parameter space that will have the maximum possible abundance in SUSY events and minimum contamination from standard model background events, a large number of candidate selection variables have been examined. The ones that show the greatest discriminating power between the SUSY signatures of interest (multiple top quarks and undetected particles in the final state) and SM events, and the least degree of correlation among themselves are the following: the number of jets, the number of b-tagged jets, the missing transverse energy, and the η of the two leading jets. The set of criteria which yield the maximum sensitivity in the SMS "T1tttt" parameter space are summarized in Table 1, and have been decided after a variety of optimization studies using simulated events.

Table 1: Selection criteria for the definition of signal region

Variable	Description	Criterion
$\not\!\!E_T$	Missing transverse energy	> 180 GeV
N_{jets}	Number of jets	> 4
$N_{\text{b-jets}}$	Number of b-tagged jets	> 2
Jet1 $\lvert\eta\rvert$	Leading jet η	< 1
Jet2 $\lvert\eta\rvert$	Sub-leading jet η	< 1

In Fig.1 the distributions of the discriminating variables for the signal (SMS "T1tttt") and the SM background events are shown, normalized to unit area, where all the selection criteria have been applied, except the one on the variable shown. The $\not\!\!E_T$ selection has been relaxed and set at 100 GeV for these plots, and two example SMS points are used : one with ($m_{\tilde{g}}$=1150 GeV, m_{LSP}=300 GeV), and another with higher LSP mass ($m_{\tilde{g}}$=1150 GeV, m_{LSP}=500 GeV).

The number of SM background and signal events for a few points in parameter space are shown in Table 2 for a total integrated luminosity of 19.7 fb^{-1}. The remaining background is composed entirely of $t\bar{t}$ events. The requirement on the number of jets eliminates 95% of the $t\bar{t}$ background,

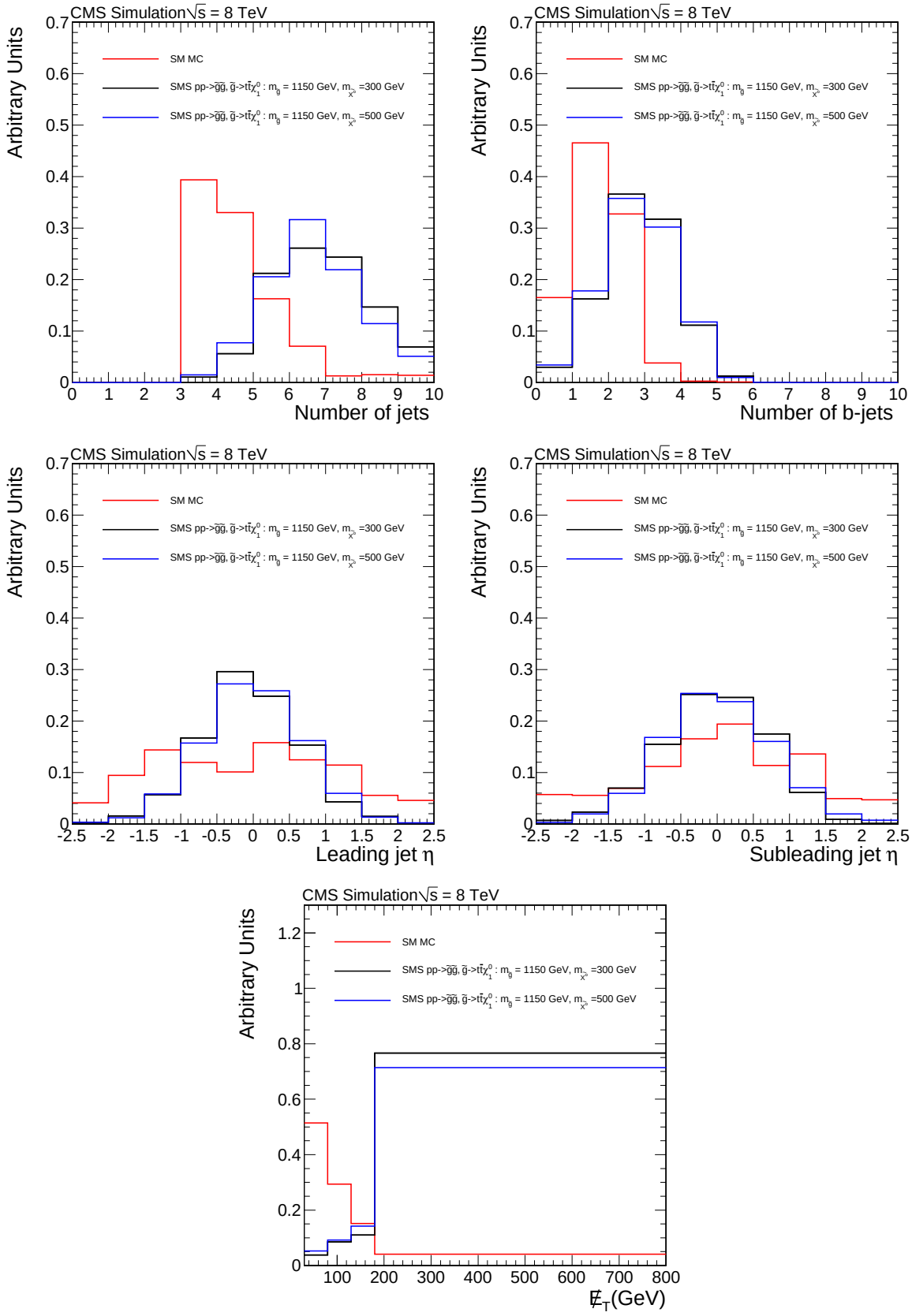

Figure 1: Discriminating variables used for signal selection for SM events (red histograms) and SMS "T1tttt" events (black histograms). Top Left: Number of jets. Top right: Number of b-tagged jets. Middle left: η of leading jet. Middle right : η of sub-leading jet. Bottom : missing transverse energy.

an additional 95% is eliminated by the requirement on the number of b-tagged jets, followed by an additional 30% eliminated by the requirement on the leading and sub-leading jet η. Finally, an additional 95% of the remaining $\mathrm{t\bar{t}}$ background is eliminated by the $\not\!\!E_{\mathrm{T}}$ criterion.

Table 2: Number of signal and background (bkg.) events predicted by simulation after the event selection criteria of two opposite-sign leptons and ≥ 2 jets, and after the signal selection criteria are applied. The uncertainties quoted are statistical only.

Sample	Event Selection	Signal selection
$\mathrm{t\bar{t}}$	82171 ± 287	2.2 ± 0.7
$\mathrm{Z}+\mathrm{jets}$	1475456 ± 1215	0.0 ± 1.5
$\mathrm{W}+\mathrm{jets}$	26978 ± 164	0.0 ± 6.3
WW	1637 ± 44	0.0 ± 0.3
WZ	1364 ± 37	0.0 ± 0.1
ZZ	3129 ± 56	0.0 ± 0.2
$\mathrm{t\bar{t}W}+\mathrm{jets}$	434 ± 3	0.2 ± 0.07
$\mathrm{t\bar{t}Z}+\mathrm{jets}$	463 ± 3	0.2 ± 0.06
Total SM Bkg.	1591632 ± 1261	2.6 ± 6.5
$m_{\tilde{\mathrm{g}}}$=1000 GeV m_{LSP}=400 GeV	28.2 ± 0.5	4.3 ± 0.2
$m_{\tilde{\mathrm{g}}}$=1150 GeV m_{LSP}=300 GeV	9.8 ± 0.2	1.9 ± 0.1
$m_{\tilde{\mathrm{g}}}$=1150 GeV m_{LSP}=500 GeV	9.5 ± 0.2	1.6 ± 0.1

4 Data-Driven Method for Background Estimation

In order to provide a robust estimate of the number of background events in the signal region, we use the data-driven method described below. The signal region (SR) is defined by the set of the signal selection requirements described in Sec. 3. A control region (CR) is defined by inverting either one of the two signal selection criteria on the η of the two leading jets. This region is chosen so that it is dominated by SM processes. Signal contamination in the control region varies with the gluino mass ($m_{\tilde{\mathrm{g}}}$) and the LSP mass (m_{LSP}). For an SMS point with ($m_{\tilde{\mathrm{g}}}$=1150 GeV, m_{LSP}=300 GeV) there are 6.3 expected SM events in the control region and the signal contamination is of the order of 10%.

Next, an extrapolation factor, $R_{\mathrm{ext.}} = \frac{N_{nb,SR}}{N_{nb,CR}}$, is defined, in bins of $\not\!\!E_{\mathrm{T}}$ and for a given b-jet multiplicity, nb, as the ratio of the number of events (for the SM-only hypothesis) in the signal region to that of the control region. The extrapolation factor, $R_{\mathrm{ext.}}$, exhibits a smooth behavior as a function of $\not\!\!E_{\mathrm{T}}$, as shown in Fig. 2 using simulated events, and furthermore it is almost invariant under the number of b-tagged jets in the events. The latter allows for $R_{\mathrm{ext.}}$ to be obtained directly from data using the events with exactly two b-tagged jets, leaving the rest of the signal and control selection criteria the same. This has the advantage of an entirely data-driven background estimation methodology which minimizes systematic uncertainties.

of the $R_{\mathrm{ext.}}$,

Combining the above the SM background prediction in the signal region is obtained as follows:

$$N^{SR}_{Predicted} = R^{Data,nb=2}_{\mathrm{ext.}} \times N^{CR}_{Data} \tag{1}$$

In Table 3 the signal and control region criteria are summarized, along with the ones used for the extrapolation ratio.

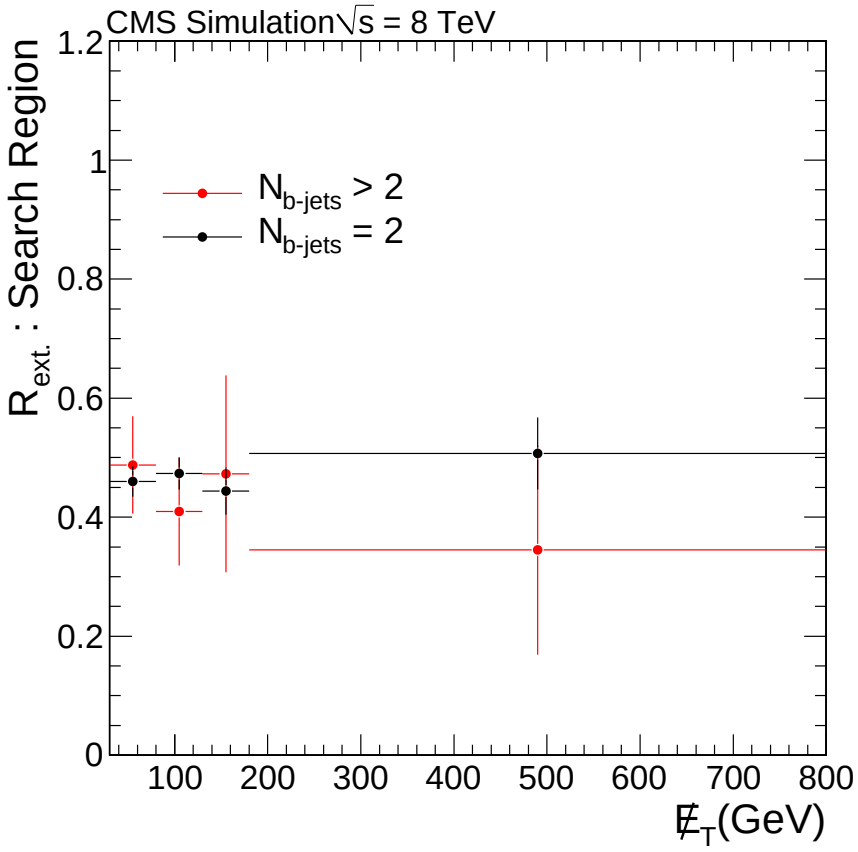

Figure 2: Extrapolation factors $R_{ext.}$ as a function of $\not{E}_{\mathrm{T}}$ for the search region (red), defined as the one with number of b-tagged jets greater than two, and for the events with two b-tagged jets.

Table 3: Definitions of control and signal regions of the data samples used in the analysis.

Region	$\not\!\!E_{\mathrm{T}}$	Number of jets	Number of b-tagged jets	Jet $\lvert\eta\rvert$
Signal	> 180 GeV	> 4	> 2	Jet1 $\lvert\eta\rvert < 1$, Jet2 $\lvert\eta\rvert < 1$
Control	> 180 GeV	> 4	> 2	Jet1 $\lvert\eta\rvert \geq 1$ or Jet2 $\lvert\eta\rvert \geq 1$
Signal for R_{ext}.	> 180 GeV	> 4	$= 2$	Jet1 $\lvert\eta\rvert < 1$, Jet2 $\lvert\eta\rvert < 1$
Control for R_{ext}.	> 180 GeV	> 4	$= 2$	Jet1 $\lvert\eta\rvert \geq 1$ or Jet2 $\lvert\eta\rvert \geq 1$

4.1 Definition of cross check region

In order to test the procedure for obtaining the SM background prediction in the signal region, described in the previous section, using both data and simulated events, cross check regions are defined using lower jet multiplicities. In the cross check regions no (very little) signal is expected in either the control or the signal region allowing for the validity of the method to be tested with data as well as simulated events. The cross check region is defined as shown in Table 4.

Table 4: Definition of the cross check region (CCR)

.

Region	$\not\!\!E_{\mathrm{T}}$	Number of jets	Number of b-tagged jets	Jet $\lvert\eta\rvert$
Signal	> 180 GeV	> 2 and ≤ 4	> 2	Jet1 $\lvert\eta\rvert < 1$, Jet2 $\lvert\eta\rvert < 1$
Control	> 180 GeV	> 2 and ≤ 4	> 2	Jet1 $\lvert\eta\rvert \geq 1$ or Jet2 $\lvert\eta\rvert \geq 1$
Signal for R_{ext}.	> 180 GeV	≥ 2 and ≤ 4	$= 2$	Jet1 $\lvert\eta\rvert < 1$, Jet2 $\lvert\eta\rvert < 1$
Control for R_{ext}.	> 180 GeV	≥ 2 and ≤ 4	$= 2$	Jet1 $\lvert\eta\rvert \geq 1$ or Jet2 $\lvert\eta\rvert \geq 1$

The extrapolation factor in the cross check region exhibits the same characteristics as in the search region as seen in Fig. 3. Namely, it shows a smooth, and almost flat behavior as a function of $\not\!\!E_{\mathrm{T}}$, and furthermore it is almost invariant under the number of b-tagged jets in the events.

4.2 Closure in data and simulation

The validity (closure) of the background prediction methodology using simulated events can be checked for the search region, as well as the cross check region. The closure using data can be examined in the cross check region. In Table 5 the predicted and observed number of events are shown for data and simulated events for the search and cross check regions. Given the uncertainties (statistical only), predictions and observations agree indicating the success of the background prediction methodology. In Fig. 4 the predicted and observed $\not\!\!E_{\mathrm{T}}$ distributions for the search and cross check regions are shown as well.

Table 5: Predicted and observed number of SM background events in the signal region of the search and cross check regions.

Region	Sample	Prediction	Observation
Cross check	MC	4.0 ± 0.8	3.7 ± 0.9
Cross check	Data	4.6 ± 2.0	$3.0^{+2.3}_{-1.3}$
Search	MC	2.8 ± 0.6	2.2 ± 0.6

4.3 Systematic uncertainties

The systematic uncertainty on the background procedure is evaluated using a series of closure tests in simulation and data, as described in the previous section. In these tests, we find good agreement between the predictions of the method and the true background yields. Due to the

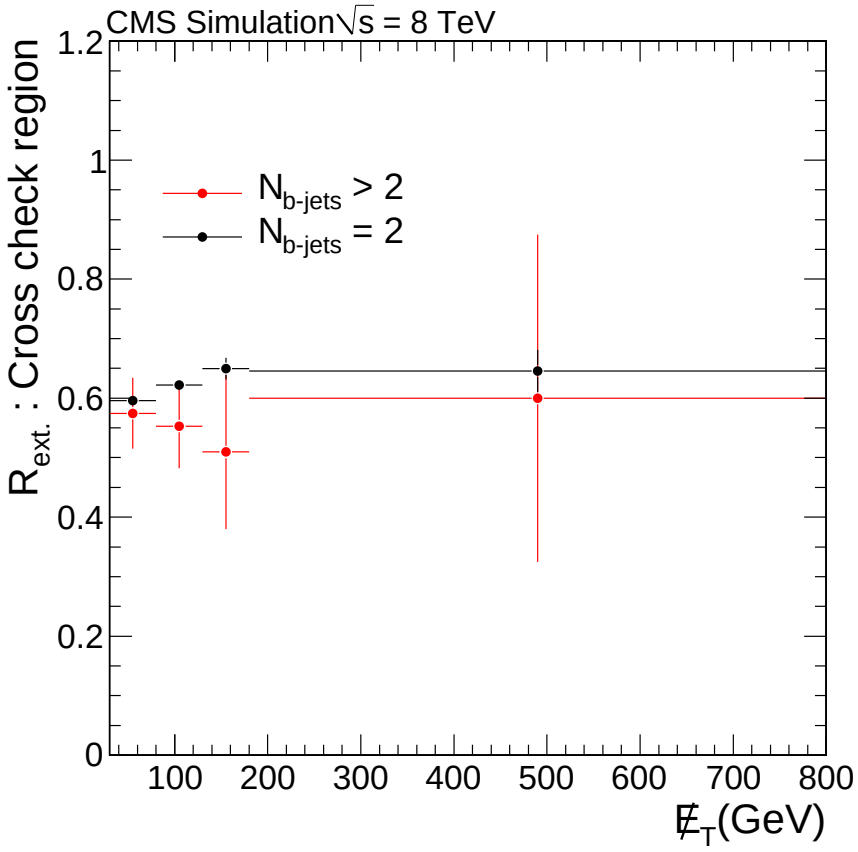

Figure 3: Extrapolation factor $R_{ext.}$ for the cross check region as a function of $\not{E}_{\mathrm{T}}$ for the search region (red) defined as the one with number of b-tagged jets greater than two, and the events with two (black) and one (blue) b-tagged jets.

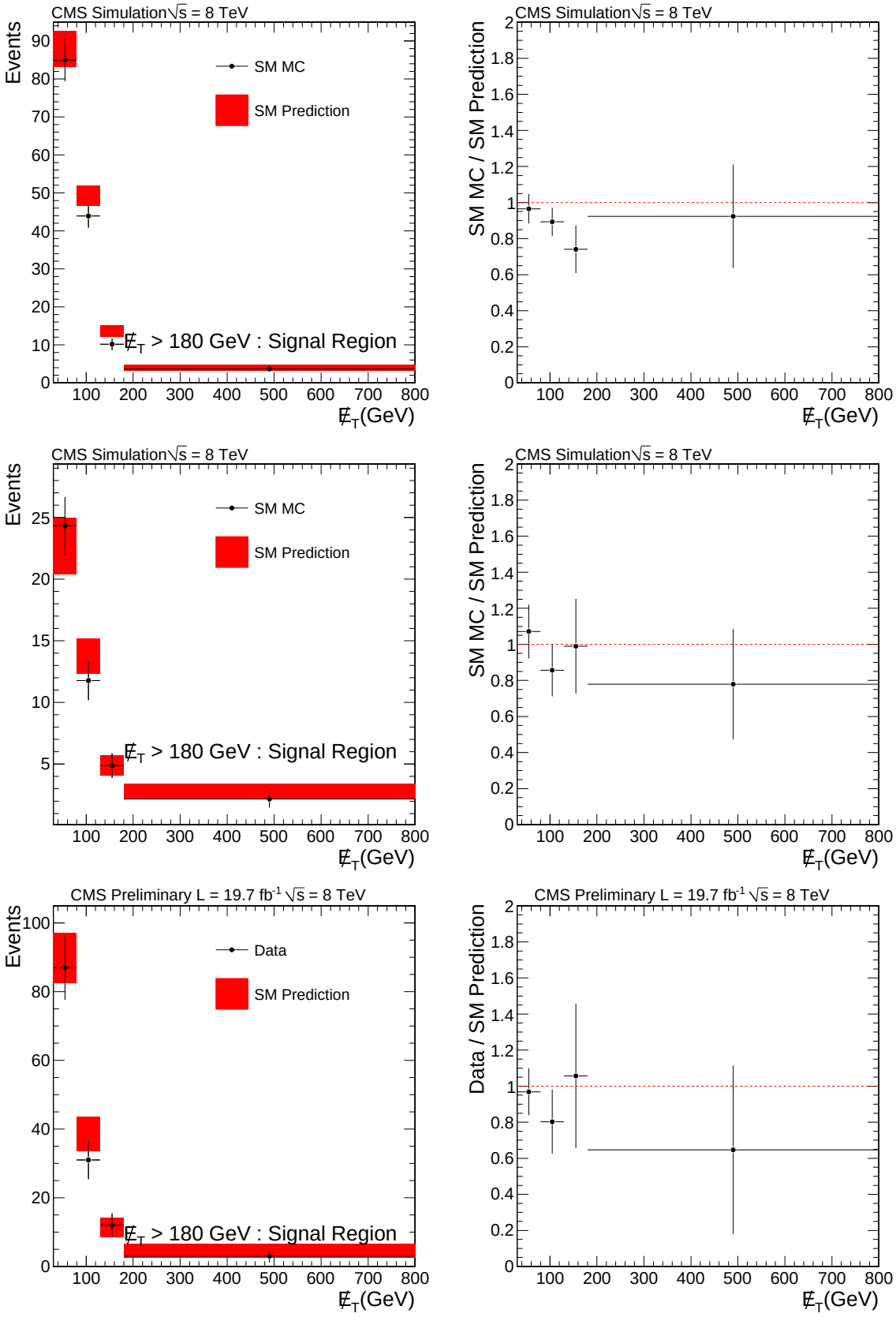

Figure 4: Comparison between predicted (red bands) and observed (black points) $\not\!\!E_T$ distributions, along with their ratios, for simulated events in the cross check region (top row), for simulated events in the search region (middle row), and for data events in the cross check region (bottom row).

large statistical uncertainties on these tests, we conservatively assign a 50% systematic uncertainty on the background prediction. The total uncertainty on the final background prediction is dominated by the limited statistical precision of the control sample.

5 Results

The number of predicted and observed events in the signal region, for an integrated luminosity of 19.7 fb^{-1}, are shown in Table 6. Table 6 also gives the model-independent 95% C.L. upper limits on the number of events in the signal region, assuming no signal contamination. The predicted and observed $\not\!\!E_{\mathrm{T}}$ distributions are shown in Fig. 5.

Table 6: Number of predicted and observed events in the signal region of the search region for an integrated luminosity of 19.7 fb^{-1}. The 95% upper limits (UL) on events produced by SUSY processes are also shown.

Predicted	Observed	95% UL expected	95% UL observed
1.20 ± 0.86 (stat.) $\pm$ 0.60 (syst.)	1	3.9	4.0

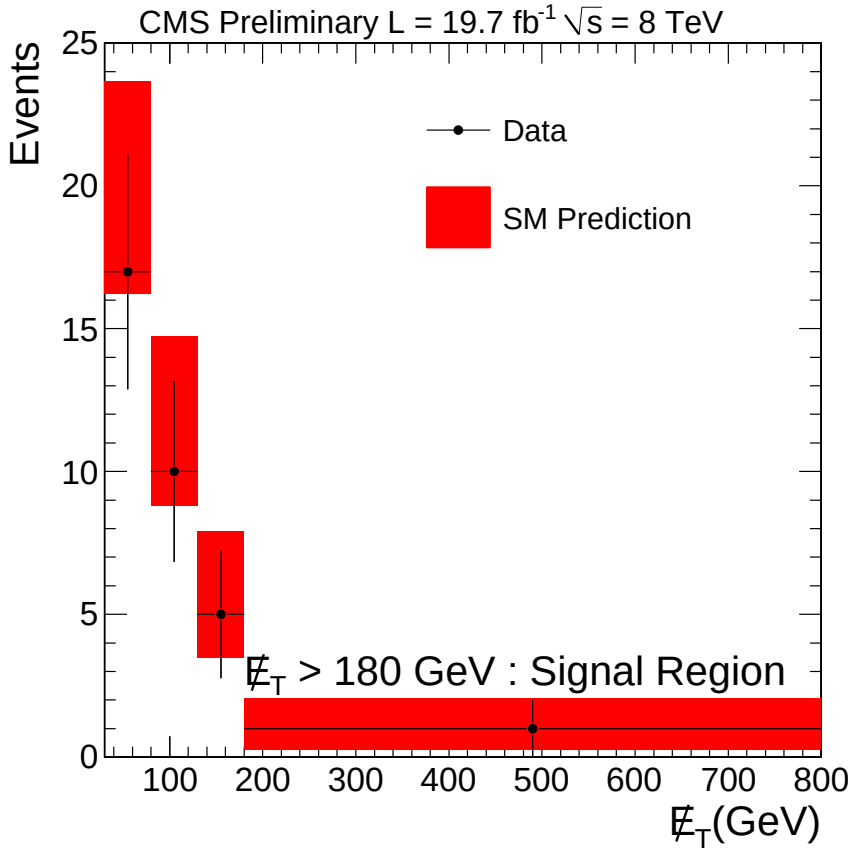

Figure 5: Comparison between predicted (red bands) and observed (black points) $\not\!\!E_{\mathrm{T}}$ distributions for data events in the signal region.

The systematic uncertainties on the signal selection are described in Table 7. The systematic uncertainty on the total integrated luminosity is 2.6% [25]. The lepton selection, reconstruction and isolation efficiency measured in data and simulated Z events, has a total uncertainty of

4%. The trigger efficiency, after applying the data-vs-simulation scale factors (which vary from 81% to 96%), has a 6% systematic uncertainty assigned. The total uncertainty on the b-tagging efficiency is determined by simultaneously varying the efficiencies to tag a bottom, charm, or light quark up and down by their uncertainties [24] and is estimated to be 10%. The jet energy scale and resolution uncertainty [16] is propagated to the $\not\!\!E_{\mathrm{T}}$ uncertainty and has a total effect of 8%.

The initial state radiation (ISR) systematic is computed according to standard CMS recommendations [26], and the statistics of the signal simulation are also taken into account in the calculation of the total systematic uncertainty. The ISR, pileup and simulation statistics systematic uncertainties are calculated for each grid point in the SMS plane, whereas the rest are flat across the entire SMS plane.

Table 7: Signal selection efficiency systematic uncertainties

Source	Uncertainty
Lepton triggers ($p_T > 20$ GeV)	6%
Lepton isolation, reconstruction and identification	4%
Luminosity	2.6%
b jet identification	14 %
Jet energy scale and resolution	8 %
PDF	2%
ISR	1-18%
Pileup effects	1%
Simulation statistics	2-30%
Total	17-39%

Finally, the observed and expected number of events are translated into limits on SMS parameter space. The 95% CL upper limits are computed using a LHC-Style $\mathrm{CL_s}$ method with profile likelihood test statistics, and lognormal distributions for the background expectation [27, 28]. The uncertainties in the NLO+NLL cross sections from the parton distribution functions [29–33], the choice of the factorization and renormalization scale, and α_{S}, are taken into account for each point, and are evaluated according to the PDF4LHC recommendation [34]. The signal contamination in the control region is taken into account.

The exclusion limits on SMS "T1tttt" models are depicted in Fig. 6. For gluino masses below

$\sim$ 1000 GeV, LSP masses below $\sim$ 450 GeV are excluded. For gluino masses above $\sim$ 1000 GeV, no limits on the mass of LSP can be set.

6 Conclusions

A search for supersymmetry in events with two opposite-sign leptons, large number of jets, b-tagged jets, and large missing transverse energy in the final state has been presented,using the 2012 dataset collected with the CMS experiment corresponding to 19.7 fb^{-1} of total integrated luminosity. The search utilizes a powerful data-driven approach for the SM background estimation. In addition, it is unique and complementary to the ones already published by the CMS collaboration using zero, one, two of same-sign, and more than two leptons in the final state [35–39]. Agreement is observed between the expectation from the SM and the data, with no significant excess, which results in limits in the SMS ($m_{\tilde{g}}, m_{\mathrm{LSP}}$) plane.

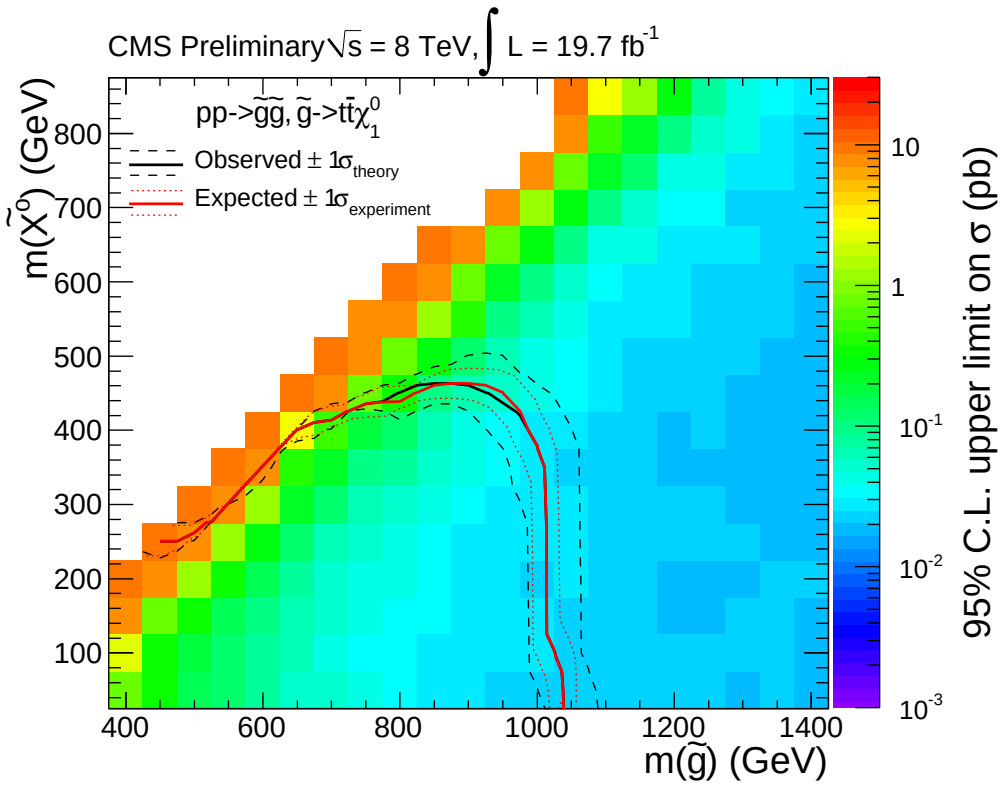

Figure 6: The 95% CL exclusion limits on the simplified model scenarios. The 95% CL upper cross section observed limit is shown for different gluino and LSP masses.

References

[1] Y. A. Golfand and E. P. Likhtman, "Extension of the Algebra of Poincaré Group Generators and Violation of p Invariance", *JETP Lett.* **13** (1971) 323.

[2] J. Wess and B. Zumino, "Supergauge transformations in four dimensions", *Nucl. Phys. B* **70** (1974) 39, doi:10.1016/0550-3213(74)90355-1.

[3] H. P. Nilles, "Supersymmetry, Supergravity and Particle Physics", *Phys. Reports* **110** (1984) 1, doi:10.1016/0370-1573(84)90008-5.

[4] H. E. Haber and G. L. Kane, "The Search for Supersymmetry: Probing Physics Beyond the Standard Model", *Phys. Reports* **117** (1987) 75, doi:10.1016/0370-1573(85)90051-1.

[5] R. Barbieri, S. Ferrara, and C. A. Savoy, "Gauge Models with Spontaneously Broken Local Supersymmetry", *Phys. Lett. B* **119** (1982) 343, doi:10.1016/0370-2693(82)90685-2.

[6] S. Dawson, E. Eichten, and C. Quigg, "Search for Supersymmetric Particles in Hadron - Hadron Collisions", *Phys. Rev. D* **31** (1985) 1581, doi:10.1103/PhysRevD.31.1581.

[7] E. Witten, "Dynamical Breaking of Supersymmetry", *Nucl. Phys. B* **188** (1981) 513, doi:10.1016/0550-3213(81)90006-7.

[8] S. Dimopoulos and H. Georgi, "Softly Broken Supersymmetry and SU(5)", *Nucl. Phys. B* **193** (1981) 150, doi:10.1016/0550-3213(81)90522-8.

[9] N. Arkani-Hamed et al., "MARMOSET: The Path from LHC Data to the New Standard Model via On-Shell Effective Theories", (2011). arXiv:hep-ph/0703088.

[10] D. Alves et al., "Simplified models for LHC new physics searches", *J. Phys. G* **39** (2012) 105005, doi:10.1088/0954-3899/39/10/105005.

[11] CMS Collaboration, "Interpretation of searches for supersymmetry with simplified models", (2013). arXiv:1301.2175.

[12] CMS Collaboration, "Performance of CMS muon reconstruction in pp collision events at $\sqrt{s} = 7$ TeV", *JINST* **7** (2012) P10002, doi:10.1088/1748-0221/7/10/P10002.

[13] CMS Collaboration, "Electron Reconstruction and Identification at $\sqrt{s} = 7$ TeV", CMS Physics Analysis Summary CMS-PAS-EGM-10-004, (2010).

[14] M. Cacciari, G. P. Salam, and G. Soyez, "The anti-k_t jet clustering algorithm", *JHEP* **04** (2008) 063, doi:10.1088/1126-6708/2008/04/063.

[15] CMS Collaboration, "Particle–Flow Event Reconstruction in CMS and Performance for Jets, Taus, and $E_{\mathrm{T}}^{\mathrm{miss}}$", CMS Physics Analysis Summary CMS-PAS-PFT-09-001, (2009).

[16] CMS Collaboration, "Determination of jet energy calibration and transverse momentum resolution in CMS", *J. Instrum.* **6** (2011) P11002, doi:10.1088/1748-0221/6/11/P11002.

[17] J. Alwall et al., "MadGraph/MadEvent v4: the newweb generation", *JHEP* **09** (2007) 028, doi:10.1088/1126-6708/2007/09/028.

[18] T. Sjöstrand, S. Mrenna, and P. Z. Skands, "PYTHIA 6.4 physics and manual", *JHEP* **05** (2006) 026, doi:10.1088/1126-6708/2006/05/026.

[19] R. Field, "Early LHC Underlying Event Data-Findings and Surprises", (2010). arXiv:1010.3558.

[20] S. Kretzer, H. Lai, F. Olness, and W. Tung, "Cteq6 parton distributions with heavy quark mass effects", *Phys. Rev. D* **69** (2004) 114005, doi:10.1103/PhysRevD.69.114005.

[21] S. Agostinelli et al., "GEANT4—a simulation toolkit", *Nucl. Instrum. Meth. A* **506** (2003) 250, doi:10.1016/S0168-9002(03)01368-8.

[22] CMS Collaboration, "Tracking and Primary Vertex Results in First 7 TeV Collisions", CMS Physics Analysis Summary CMS-PAS-TRK-10-005, (2010).

[23] CMS Collaboration, "Calorimeter Jet Quality Criteria for the First CMS Collision Data", CMS Physics Analysis Summary CMS-PAS-JME-09-008, (2010).

[24] CMS Collaboration, "Identification of b-quark jets with the CMS experiment", *JINST* **8** (2013) P04013, doi:10.1088/1748-0221/8/04/P04013.

[25] CMS Collaboration, "CMS Luminosity Based on Pixel Cluster Counting -Summer 2013 Update", CMS Physics Analysis Summary CMS-PAS-LUM-13-001, (2013).

[26] CMS Collaboration, "Search for top-squark pair production in the single-lepton final state in pp collisions at $\sqrt{s}$ = 8 TeV", (2013). arXiv:1308.1586.

[27] A. L. Read, "Presentation of search results: the CL_s technique", *J. Phys. G* **28** (2002) 2693, doi:10.1088/0954-3899/28/10/313.

[28] T. Junk, "Confidence level computation for combining searches with small statistics", *Nucl. Instrum. Meth. A* **434** (1999) 435, doi:10.1016/S0168-9002(99)00498-2.

[29] M. Krämer et al., "Supersymmetry production cross sections in pp collisions at $\sqrt{s}$ = 7 TeV", (2012). arXiv:1206.2892.

[30] W. Beenakker, R. Höpker, M. Spira, and P. M. Zerwas, "Squark and gluino production at hadron colliders", *Nucl. Phys. B* **492** (1997) 51, doi:10.1016/S0550-3213(97)80027-2.

[31] A. Kulesza and L. Motyka, "Threshold Resummation for Squark-Antisquark and Gluino-Pair Production at the LHC", *Phys. Rev. Lett.* **102** (2009) 111802, doi:10.1103/PhysRevLett.102.111802.

[32] A. Kulesza and L. Motyka, "Soft gluon resummation for the production of gluino-gluino and squark-antisquark pairs at the LHC", *Phys. Rev. D* **80** (2009) 095004, doi:10.1103/PhysRevD.80.095004.

[33] W. Beenakker et al., "Soft-gluon resummation for squark and gluino hadroproduction", *JHEP* **12** (2009) 041, doi:10.1088/1126-6708/2009/12/041.

[34] S. Alekhin et al., "The PDF4LHC Working Group Interim Report", (2011). arXiv:1101.0536.

[35] CMS Collaboration, "Search for gluino-mediated bottom- and top-squark production in pp collisions at 8 TeV", *Phys.Lett.B* **725** (2013) 243, doi:10.1016/j.physletb.2013.06.058.

[36] CMS Collaboration, "Search for supersymmetry in hadronic final states with missing transverse energy using the variables AlphaT and b-quark multiplicity in pp collisions at 8 TeV", *Eur. Phys. J. C* **73** (2013) 2568, doi:10.1140/epjc/s10052-013-2568-6.

[37] CMS Collaboration, "Search for supersymmetry using events with a single lepton, multiple jets, and b-tags", CMS Physics Analysis Summary CMS-PAS-SUS-13-007, (2013).

[38] CMS Collaboration, "Search for new physics in events with same-sign dileptons and jets in pp collisions at $\sqrt{s}$ = 8 TeV", CMS Physics Analysis Summary CMS-PAS-SUS-13-013, (2013).

[39] CMS Collaboration, "Search for supersymmetry in the 3 lepton + b-tag final state in pp collisions at 8 TeV", CMS Physics Analysis Summary CMS-PAS-SUS-13-008, (2013).